Stability-Constrained Optimization for Energy Efficiency in Polling-Based Wireless Networks

Yi Xie
Department of Computing
The Hong Kong Polytechnic University
Hong Kong, SAR China
csyxie@comp.polyu.edu.hk

Rocky K. C. Chang
Department of Computing
The Hong Kong Polytechnic University
Hong Kong, SAR China
csrchang@comp.polyu.edu.hk

ABSTRACT

A wireless device's energy can be saved by putting it into the sleeping mode (power saving mode, PSM) or decreasing its transmission power (transmission power control, TPC) which prolongs the packet transmission time. However, decreasing one's transmission power would prevent others from transmitting their packets. Clearly, there are complex interactions when each tries to optimize its own energy efficiency. Therefore, in this paper we are considering the problem of optimizing the energy efficiency for *all* wireless devices in the network with the constraint that they are all stable. In particular, we consider the polling-based MAC protocols with phase grouping and mobile grouping schedules, and we employ both the PSM and TPC to save the energy. We have formulated stability-constrained optimization problems for them, and have proposed an iterative algorithm to compute the optimal power allocations for the wireless devices. We have conducted a lot of experiments to validate the accuracy of the algorithm and to evaluate the gains in the energy efficiency for the two schedules. The mobile grouping schedule is found to be much more energy efficient than the PG schedule, especially when the downlink traffic is higher than the uplink traffic. We have also studied the impact of the optimized schedules on the delay performance.

1. INTRODUCTION

Energy efficiency is one of the important design issues to consider in wireless networks. Various mechanisms have been proposed to trade-off between energy consumption and the communication quality [1]. In this paper we mainly concentrate on the media access control (MAC) sublayer in a wireless infrastructure network in which an access point (AP) serves as the relay for a number of wireless clients. The wireless MAC protocols can be based on random access or coordinated access. For example, in the IEEE 802.11 wireless LAN, the standard prescribes the distributed coordinated function (DCF) and point coordinated function (PCF). The DCF is based on Carrier Sense Multiple Access with Collision Avoidance (CSMA/CA) and the PCF is mainly based on a polling scheme.

In this paper we consider the polling-based MAC protocol for a wireless LAN. The polling-based MAC provides a number of advantages over the random access MAC. For example, it can guarantee a certain level of quality-of-service to each client even when the channel is accessed simultaneously by multiple clients. As we shall see in this paper, the polling-based MAC can also be used to optimize the energy consumption of the entire wireless LAN. We will employ 2 mechanisms to reduce the energy consumption—the power saving mode (PSM) and the transmission power control (TPC) [2]. The PSM reduces the energy consumption by putting wireless devices into the sleeping mode (e.g. [3]), while the TPC reduces the transmission power to conserve energy.

The TPC is based on the fact that the communication energy can be saved by transmitting packets over a longer duration, i.e., reducing the transmission rate [4]. We adopt the TPC with the convex rate-power curve derived from the Shannon's theorem. First, the ideal channel capacity is given by $C_{max} = W \times \log_2(1 + \frac{S}{N})$ bps, where W is the bandwidth in Hz, N is the Gaussian noise power, and S is the signal power. The transmission rate R is given by αC_{max} bps, where $\alpha \in (0, 1)$, depicts the ratio of the real channel capacity to C_{max}. By introducing an attenuation factor A, which is the ratio of the transmission power P to S, the power-rate relationship (1) is shown in Figure 1(a).

$$R = \alpha W \log_2(1 + P/(AN)). \quad (1)$$

Moreover, the energy spent on transmitting 1 bit, $e(t) = tP$, is a convex function of its transmission time $t = \frac{1}{R}$. Therefore, $e(t)$ can be reduced by lowering P, which results in a smaller R and a longer t. The relationship is illustrated in Figure 1(b).

Most of the power-saving mechanisms, including the PSM and TPC, will nevertheless degrade the communication and application performance. Therefore, many previous works considered optimal trade-offs between energy consumption and various performance metrics, such as throughput [5], delay [6, 7, 8], network utility [9], and error rate [2, 10]. Moreover, the previous works considered the trade-offs for individual wireless device and did not consider how the individual energy-saving actions affect each other. This paper addresses the energy consumption problem for the entire network. In other words, an individual device cannot slow

Valuetools '06, October 11-13, 2006, Pisa, Italy

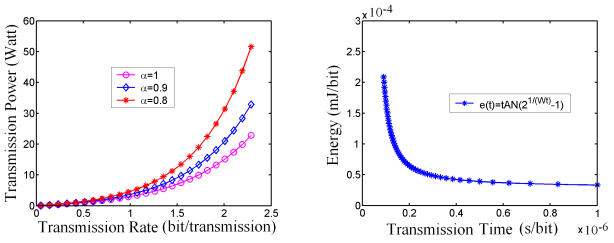

(a) Power-rate curves (b) Energy-time curves

Figure 1: Trade-off of energy & transmission rate

its transmission rate to the extent that other devices would be starved. As a result, we will optimize the total energy consumption of all devices under the constraints that all the devices are stable, i.e., stability-constrained optimization. By stability, we mean that the queue length would not grow unbounded. Moreover, we will consider 2 polling schedules—phase grouping and mobile grouping, and compare their performance in terms of the energy efficiency.

2. RELATED WORK

The phase grouping schedules have been widely deployed. The typical example is the energy conserving MAC (EC-MAC) protocol [10] which uses an explicit transmission order with reservations. In the broadcast (downlink) phase, the wireless device listens to the downlink for the transmission order. The AP's centralized scheduler tries to reduce the energy consumption and support QoS in the uplink phase. Many mobile grouping polling-based protocols have also been proposed to minimize the energy consumption by having less transitions, and control the packet transmission [11], such as the disposable token MAC Protocol (DTMP) [12], the E^2MaC protocol [13], and the mobile grouping schedule [14].

Moreover, a number of mechanisms have been proposed to trade-off between energy efficiency and other performance metrics. Some packet transmission schedules in wireless communications are designed to minimize the energy consumption subject to the deadline or the delay constraint, e.g., the optimal offline/online schedules [15] and the Move-right algorithm [16]. Cross-layer schemes are proposed to balance the reduction of delay (transmission time) and the energy conservation, e.g., the energy-efficient PCF [2] for uplink data transmission. It controls the transmission rate by the PHY rate adaptation, while uses the TPC to select the best transmit power level to combat the co-channel interference. According to the given power-rate function, the TPC may determine the most energy efficient transmission strategy for each data frame, e.g. an optimal rate-power combination table in Miser [17]. Besides, Zhang and Chanson have attempted to minimize the energy consumption subject to the given throughput constraints, or maximize the throughput subject to a fixed energy storage [5]. Chiang and Bell defined network utility based on all user utilities, and studied the problem of maximizing the network utility with energy constraints [9]. Nuggenhalli et al designed a delay constrained transmission schedule that maximizes the lifetime of a transmitter [7], and further took the energy recovery property of batteries into consideration [18].

Instead of considering specific performance metrics, we consider the guarantee of stability as a foundation requirement for wireless communication. The solution of our stability-constrained energy minimization problem is the optimal transmission power allocations, which is easy to deploy in wireless nodes. That is, our optimal transmission power allocations have provided a stable network consuming energy efficiently. When wireless applications require specific performances, e.g. a short delay or a large throughput, other energy efficient schemes may be applied as the complementary part of our design.

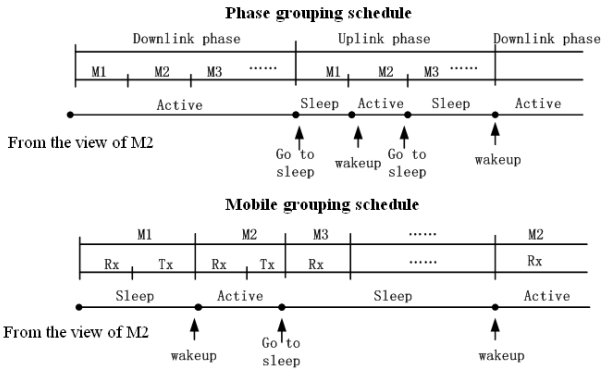

Figure 2: Grouping schedules of polling-based MAC

The rest of the paper is organized as follows. In the next section, we describe the 2 polling schedules and model them using cyclic-service queueing models. In section 4, we formulate stability-constrained optimization problems for the 2 schedules. Then we compute optimal solutions and present an iterative algorithm in section 5. In section 6, we first evaluate the performance of the iterative algorithm and then compare the energy efficiency of the 2 schedules. We have also evaluated the impact of the PSM and TPC on the delay performance. We finally conclude this paper with future directions in section 7.

3. SYSTEM MODELS

We consider 2 types of polling schedules—*phase grouping* (PG) schedule and *mobile grouping* (MG) schedule. In the PG schedule, the uplink and downlink phases alternate between them, as illustrated in Figure 2. In the downlink phase, the AP broadcasts packets to all wireless devices $M1$, $M2$, ... Thus, all devices have to stay active in order to receive their packets. However, each device is polled individually in the uplink phase. Therefore, using the PSM, a device can be put into the sleeping mode when it is not polled, and be awaken into the active mode when it is polled during the uplink phase. On the other hand, the MG schedule groups the uplink and downlink phases for each wireless device, e.g. [12]. Each device stays in the sleeping state except when it is polled by the AP for message reception and transmission. Note that frequent transitioning between the sleeping mode and the active mode also consumes a significant amount of energy.

We model the MG and PG schedules using a cyclic-service queueing model [19]. We first describe the common model elements here, and then continue the model description that differs for these two schedules. Consider that there are c wireless devices in the network, which are serviced by an AP according to a fixed polling schedule. Each wireless de-

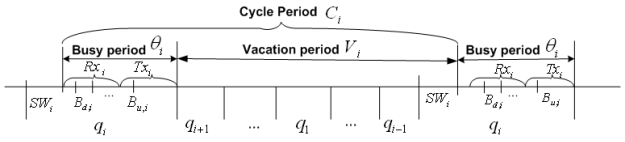

Figure 3: A queueing model for the MG schedule

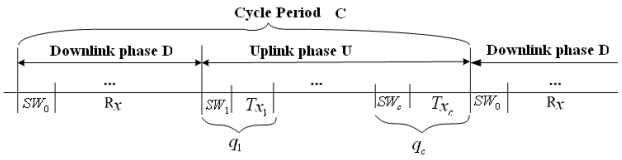

Figure 4: A queueing model for the PG schedule

vice is modeled as a queue with infinite buffers, denoted by q_i $(i = 1, \ldots, c)$, and the AP is modeled as a server. The server will leave the polled queue when it is empty or when all packets arrived before the server visits have been serviced. Packets are generated at the queues for uplink transmissions to the AP, and packets are generated at the AP for downlink transmissions to the queues. The arrival processes of the uplink traffic and downlink traffic are assumed to be independent Poisson processes, with mean arrival rates equal to $\lambda_{u,i}$ and $\lambda_{d,i}$ for q_i, respectively. The total arrival process of q_i is therefore also Poisson with rate $\lambda_i = \lambda_{u,i} + \lambda_{d,i}$. The uplink (downlink) service time processes, which are assumed to be independent and generally distributed, are denoted as $B_{u,i}(B_{d,i})$ for q_i, with mean equal to $b_{u,i}(b_{d,i}) < \infty$. Note that the mean service times are not constants due to the TPC scheme.

In the model for the MG schedule, the server visits each queue in a deterministic and cyclic order: $q_1, q_2, \ldots, q_c, q_1, \ldots$. The downlink traffic is assigned a higher priority over the uplink traffic in all queues. Moreover, there is a nonzero walk time involved in switching between queues, which is modeled as the wake-up period. The walk time process from q_{i-1} to q_i, denoted by SW_i, is generally distributed with mean $s_i < \infty$, and the walk time processes are independent of each other. In addition, we define several quantities that are useful for our discussion later. Consider a target queue in the system q_i. From q_i's point of view, the server is either serving it or is on vacation, as shown in Figure 3. We define the period, in which the server is serving q_i, as q_i's *busy period*, denoted by Θ_i. The busy period is further divided into a uplink period Tx_i and a downlink period Rx_i. On the other hand, the period, in which the server is away from q_i, is called the *vacation period* (from q_i's viewpoint), denoted by V_i. The *cycle time* C_i is given by a sum of Θ_i and V_i.

The model for the PG schedule depicted in Figure 4 is similar to the one for the MG schedule, except that we separate the downlink and uplink phases. The sum of all Tx_i and SW_i is regarded as the uplink phase, during which the server visits the queues in the fixed order. The uplink periods Tx_i are defined similarly as before. The walk time process SW_i models the time spent on switching from one queue to another, which is usually a small amount of time. Unlike the MG schedule, the AP transmits all packets with the same transmission power and the same average transmission time $\overline{b_D}$. Therefore, the downlink phase is modeled as another queue with traffic generated by the AP. A walk time SW_0 is spent before all wireless devices are ready to receive data, which is generally distributed with the mean s_0. The length of the downlink phase equals to the sum of the downlink period Rx and SW_0. The cycle time C is defined as the sum of the uplink phase and the downlink phase.

In Table 1, we present the three different energy-consuming modes for the MG and PG schedules. In the active mode, we separate the transmission and reception periods. Normally, the relative power consumption for the 3 modes are given by: $P_{V,i} \ll P_{I,i}$ and $P_{Rx,i} < P_{Tx,i}$.

Table 1: Power modes in the MG and PG schedules

System model	Scheme	Notation	Mode, power
q_i's transmission	MG, PG	Tx_i	Active, $P_{Tx,i}$
q_i's reception	MG	Rx_i	Active, $P_{Rx,i}$
Receiving period	PG	Rx	Active, P_{Rx}
q_i's state transition	MG	SW_i	Wake-up, $P_{I,i}$
	PG	SW_0, SW_i	
q_i's sleep period	MG	$V_i - SW_i$	Sleep, $P_{V,i}$
	PG	$C - SW_0 - Rx$ $-SW_i - Tx_i$	

4. STABILITY-CONSTRAINED OPTIMIZATION PROBLEMS

Let E_i be the energy consumed by q_i during a cycle. We are interested in computing the average of $E = \sum_{j=1}^{c} E_j$ for the MG and PG schedules. According to the Law of Large Numbers, the statistical average converges to its expectation, $\mathbf{E}[E]$. As for the power constraint, the wireless devices are assumed to operate within $[P_{min}, P_{max}]$. Besides, let the AP's transmission power when sending data to q_i be $P_{AP,i}$ $(\leq P_{MAX})$. The second set of constraints are on the device (queue) stability which is defined in the following [20].

DEFINITION 1. *The device q_i is considered* stable *if the distribution of queue length $L(t)$ converges to some proper distribution F, i.e.*

$$\lim_{t\to\infty} Pr\{L(t) < x\} = F(x), \lim_{x\to\infty} F(x) = 1.$$

q_i is called substable if $\lim_{x\to\infty} \lim_{t\to\infty} \inf Pr\{L(t) < x\} = 1.$

A network is considered stable if all the nodes in the network are substable; it is considered unstable otherwise. From the analysis results of [21], the total workload $\rho = \sum_{i\forall} \lambda_i b_i$ must be strictly less than 1, if the whole network is stable. In order to apply the standard optimization problem formulation, we relax the stability constraint to $\rho \leq 1$. The relaxation on the stability constraint in practice does not affect the optimization results, because all the experiments performed show that none of the optimal solutions are on the stability boundary.

4.1 The mobile grouping schedule

Consider q_i in the MG schedule. E_i consists of the energy consumption during the sleep state, the transition from the sleep state to the active state, and the active mode (transmit and receive). That is, $E_{MG,i} = P_{Tx,i}Tx_i + P_{Rx,i}Rx_i + P_{I,i}SW_i + P_{V,i}(V_i - SW_i)$. Therefore, the total energy consumption of all queues in one cycle is given by $E_{MG} = \mathbf{P}_{Tx}^T\mathbf{Tx} + \mathbf{P}_{Rx}^T\mathbf{Rx} + \mathbf{P}_I^T\mathbf{SW} + \mathbf{P}_V^T(\mathbf{V} - \mathbf{SW})$, where all vectors

are of dimension c. The objective function then becomes

$$\begin{aligned}\mathbf{E}(E_{MG}) &= \mathbf{E}[\mathbf{P}_{Tx}^T\mathbf{Tx}] + \mathbf{E}[\mathbf{P}_{Rx}]^T\mathbf{E}[\mathbf{Rx}] + \\ &\quad \mathbf{E}[\mathbf{P}_I]^T\mathbf{E}[\mathbf{SW}] + \mathbf{E}[\mathbf{P_V}]^T(\mathbf{E}[\mathbf{V}] - \mathbf{E}[\mathbf{SW}]).\end{aligned}$$

Moreover, $\mathbf{E}[C]$ is the same for all queues which is given by $\sum_{j=1}^{c}(\mathbf{E}[Tx_j]+\mathbf{E}[Rx_j]+\mathbf{E}[SW_j])$. Combined with the power constraints, the optimization problem for the MG schedule is formulated as

$$\begin{aligned}\min_{\mathbf{b_d},\mathbf{b_u}} \quad & \mathbf{E}(E_{MG}) \qquad (2)\\ s.t. \quad & \sum_{j=1}^{c}(\lambda_{d,j}b_{d,j} + \lambda_{u,j}b_{u,j}) - 1 \le 0.\\ & P_{AP,i} \le P_{MAX}, \ \ \forall i.\\ & P_{min} \le P_{Tx,i} \le P_{max}, \ \ \forall i.\end{aligned}$$

4.2 The phase grouping schedule

For the PG schedule, q_i consumes energy during the entire downlink reception period, the mode transitions, the transmission period, and the sleeping period. Therefore, $E_{PG,i} = P_{Rx,i}Rx + P_{Tx,i}Tx_i + P_{I,i}(SW_0 + SW_i) + P_{V,i}(C - SW_0 - Rx - SW_i - Tx_i)$. Similar to the previous case, we can obtain the objective function for the PG schedule as

$$\begin{aligned}\mathbf{E}(E_{PG}) &= (\mathbf{E}[\mathbf{P}_{Rx}]^T\mathbf{E}[Rx] + \mathbf{E}[\mathbf{P}_I]^T\mathbf{E}[SW_0])\mathbf{I}(c,1) + \\ &\quad +\mathbf{E}[\mathbf{P}_I]^T\mathbf{E}[\mathbf{SW}] + \mathbf{E}[\mathbf{P}_{Tx}^T\mathbf{Tx}] + \mathbf{E}[\mathbf{P_V}]^T \times \\ &\quad (\mathbf{E}[C - SW_0 - Rx]\mathbf{I}(c,1) - \mathbf{E}[\mathbf{SW}] - \mathbf{E}[\mathbf{Tx}]),\end{aligned}$$

where $\mathbf{E}[C] = \mathbf{E}[Rx] + \sum_{j=1}^{c}(\mathbf{E}[Tx_j] + \mathbf{E}[SW_j])$ and $\mathbf{I}(c,1)$ is a c-dimensional identity vector, i.e. e_c. Therefore, the optimization problem for the PG schedule is formulated as

$$\begin{aligned}\min_{\mathbf{b_d},\mathbf{b_u}} \quad & \mathbf{E}(E_{PG}) \qquad (3)\\ s.t. \quad & \overline{b_D}\sum_{j=1}^{c}\lambda_{d,j} + \sum_{j=1}^{c}(\lambda_{u,j}b_{u,j}) - 1 \le 0.\\ & P_{AP,i} \le P_{MAX}, \ \ \forall i.\\ & P_{min} \le P_{Tx,i} \le P_{max}, \ \ \forall i.\end{aligned}$$

5. COMPUTING OPTIMAL POWER ALLOCATIONS

In this section we solve the stability-constrained optimization problems formulated in the last section. First, let F_i be the r.v. for q_i's packet size in terms of the number of bits. According to (1) and $SNR_i(\mathbf{P}_{Tx}) = \frac{P_{Tx,i}/g_{ii}}{N_i + \sum_{j\neq i}^{c} P_{Tx,j}g_{ij}}$ defined in [9], the uplink packet service time is given by

$$B_{u,i} = \frac{2F_i/\alpha W}{\log_2(1 + SNR_i(\mathbf{P}_{Tx}))}, \qquad (4)$$

where $\mathbf{P}_{Tx}$ is the transmission power vector for all wireless devices. Besides, g_{ij} $(i,j = 1,\ldots,c)$ denotes the attenuations/gains between the wireless channels of q_i and q_j. N_i is the noise power of the wireless channel for q_i. Similarly, the downlink packet service time $B_{d,i}$ is given by

$$B_{d,i} = \frac{2F_i/\alpha W}{\log_2(1 + SNR_i(\mathbf{P}_{AP}))}, \qquad (5)$$

where $\mathbf{P}_{AP}$ is the AP's transmission power vector.

Table 2: Results for cyclic-service queuing model

Cycle period	$\mathbf{E}[C] = \frac{s}{1-\rho}$, where $s = \sum_{j=1}^{c} s_j$, $\rho_i = \lambda_i b_i$, and $\rho = \sum_{i=1}^{c}\rho_i$
Busy period	$\mathbf{E}[\Theta_i] = \rho_i\mathbf{E}[C]$.
Vacation period	$\mathbf{E}[V_i] = (1-\rho_i)\mathbf{E}[C]$.

5.1 The mobile grouping schedule

The optimal solution to (2) consists of two optimal service time vectors $\mathbf{b_u}$ and $\mathbf{b_d}$. Our aim is to allocate $\mathbf{P^*}_{AP}$ and $\mathbf{P^*}_{Tx}$ in order to minimize the energy consumed by all devices with the assurance of stability. To make the following analysis tractable, we assume the followings.

1. Let $P_{max} = P_{MAX}$ and the transmission powers in both directions are the same, i.e. $P_i \equiv P_{Tx,i} = P_{AP,i} \in [P_{min}, P_{max}], \forall i$.
2. No interference between wireless channels, i.e. $g_{ij} = 0$, $\forall i \neq j$. By (4) and (5), we have $B_i \equiv B_{u,i} = B_{d,i}$ with mean $b_i = \frac{H_i}{\log_2(1+P_i/K_i)}$, where $K_i = g_{ii}N_i$ and $H_i = 2\mathbf{E}[F_i]/\alpha W$. Since $SNR \gg 1$, we have
$$P_i(b_i) \approx K_i \times 2^{H_i/b_i}, \forall i. \qquad (6)$$
3. All queues have the same power consumptions when receiving, transitioning and sleeping, i.e., P_R, P_I and P_V for all queues.

Denote the ratio of the downlink traffic by $\beta_i = \frac{\lambda_{d,i}}{\lambda_{d,i}+\lambda_{u,i}}$; therefore, we have $\mathbf{E}[Rx_i] = \beta_i\mathbf{E}[\Theta_i]$ and $\mathbf{E}[Tx_i] = (1-\beta_i)\mathbf{E}[\Theta_i]$. We refer the 2 special cases of $\boldsymbol{\beta} = \mathbf{1}$ and $\boldsymbol{\beta} = \mathbf{0}$ to as *pure downlink* and *pure uplink*, respectively. By applying the well-known results for the cyclic-service queueing systems [19] summarized in Table 2, the optimization problem stated in (2) becomes

$$\begin{aligned}\min_{\mathbf{b}} \quad & \frac{s\sum_{j=1}^{c}\rho_j[(1-\beta_j)P_{Tx,j} + \beta_j P_R]}{1-\rho} + s(P_I + P_V\frac{c-1}{1-\rho}),\\ s.t. \quad & \sum_{j=1}^{c}\lambda_j b_j - 1 \le 0.\\ & \frac{H_i}{\log_2(P_{max}/K_i)} - b_i \le 0, \ \forall i.\\ & b_i - \frac{H_i}{\log_2(P_{min}/K_i)} \le 0, \ \forall i. \qquad (7)\end{aligned}$$

PROPOSITION 1. *In the pure downlink case, the optimal power allocation for the MG schedule is for the AP to transmit data to all wireless nodes with the maximal power.*

PROOF. In this case, $\boldsymbol{\beta} = \mathbf{1}$, and $b_{d,i} = b_i$, $\forall i$. We adopt the Karush-Kuhn-Tucker (KKT) optimality conditions [22] to find the optimal vector of the downlink mean service times $\mathbf{b}_d^*$ and the corresponding optimal power allocation $\mathbf{P^*_{AP}}$. For a Lagrangian multiplier set $\{u^* \le 0, \mathbf{v}^* \le \mathbf{0}\}$, we have

$$\frac{\lambda_i s[P_R + P_V(c-1)]}{(1-\sum_{j=1}^{c}\lambda_j b_{d,j}^*)^2} - u^*\lambda_i + v_i^* = 0, \ \forall i. \qquad (8)$$

$$u^*(\sum_{j=1}^{c}\lambda_j b_{d,j}^* - 1) = 0. \qquad (9)$$

$$v_i^*(\frac{H_i}{\log_2(P_{MAX}/K_i)} - b_{d,i}^*) = 0, \ \forall i. \qquad (10)$$

Note that the objective function is finite if $\sum_{j=1}^{c} \lambda_j b_{d,j}^* \neq 1$; therefore from (9), $u^* = 0$. Moreover, according to (8), v_i^* is strictly less than 0. In order to satisfy (10), it is then necessary that $b_{d,i}^* = \frac{H_i}{\log_2(P_{MAX}/K_i)}$, $\forall i$. That is, the AP transmits with the maximal power. □

When the uplink traffic exists, the interaction between P_i and b_i is more complicated. Prop. 2 gives a necessary condition for an optimal solution. Moreover, the proposition serves as the basis for designing an iterative algorithm to solve the optimization problem, which will be discussed later in this section.

PROPOSITION 2. *If all wireless devices do not transmit data using their extreme power, $\mathbf{b}^*$ must satisfy $\mathbf{L}(\mathbf{b}^*) = \mathbf{R}(\mathbf{b}^*)$ in an optimal MG schedule.*

PROOF. According to the KKT conditions, $\mathbf{b}^*$ is a local minimum only when (11)-(14) are satisfied for a set of lagrangian multipliers $\{u^* \leq 0, \mathbf{v}^* \leq \mathbf{0}, \boldsymbol{\sigma}^* \leq \mathbf{0}\}$:

$$\frac{s\lambda_i[L_i(\mathbf{b}^*) - R_i(\mathbf{b}^*)]}{(1-\sum_{j=1}^{c}\lambda_j b_j^*)^2} - u^*\lambda_i + v_i^* - \sigma_i^* = 0, \ \forall i. \quad (11)$$

$$u^*(\sum_{j=1}^{c}\lambda_j b_j^* - 1) = 0. \quad (12)$$

$$v_i^*(\frac{H_i}{\log_2(P_{max}/K_i)} - b_i^*) = 0, \ \forall i. \quad (13)$$

$$\sigma_i^*(b_i^* - \frac{H_i}{\log_2(P_{min}/K_i)}) = 0, \ \forall i, \quad (14)$$

where $\rho_i = \lambda_i b_i$, $\rho = \sum_{j=1}^{c}\rho_j$, and

$$L_i(\mathbf{b}) = [(1-\beta_i)P_i(b_i) + \beta_i P_R](1-\rho) + P_V(c-1) + \sum_{j=1}^{c}\rho_j[(1-\beta_j)P_j(b_j) + \beta_j P_R], \quad (15)$$

$$R_i(\mathbf{b}) = (1-\beta_i)P_i(b_i)(1-\rho)\ln(\frac{P_i(b_i)}{K_i}). \quad (16)$$

Since $\sum_{j=1}^{c}\lambda_j b_j^* \neq 1$, it is easy to see from (12) that $u^* = 0$. If $P_{min} < P_i^* < P_{max}$, we have $v_i^* = \sigma_i^* = 0$ from (13) and (14). Lastly, based on (11), we obtain $L_i(\mathbf{b}^*) - R_i(\mathbf{b}^*) = 0 \ \forall i$. □

5.2 The phase grouping schedule

We model the downlink phase in the PG schedule as an M/G/1 queue q_0 with rate $\lambda_D = \sum_{j=1}^{c}\lambda_{d,j}$. Since the busy period distribution of this queue is the same as that for an M/G/1 queue with c priority classes, its mean transmission time is $\overline{b_D} = (1/\lambda_D)\sum_{j=1}^{c}\lambda_{d,j}b_{d,j}$ [23]. In this case, the total average walk time is $s' = s_0 + \sum_{j=1}^{c} s_j$, and the expected cycle period is $\mathbf{E}[C] = \frac{s'}{1-\rho'}$, where the total workload $\rho' = \sum_{j=1}^{c}\rho_{u,j} + \rho_D$, $\rho_{u,i} = \lambda_{u,i}b_{u,i}$, and $\rho_D = \lambda_D\overline{b_D}$. Furthermore, the expected receiving period $\mathbf{E}[Rx]$ is the busy period of q_0, i.e., $\rho_D\mathbf{E}[C]$. The expected transmission period of q_i is $\mathbf{E}[Tx_j] = \rho_{u,j}\mathbf{E}[C]$. Using (4), (5), the results in Table 2, and assuming that P_R, P_I, and P_V are constants, the optimization problem for the PG schedule becomes

$$\begin{aligned}
\min_{\mathbf{b_d},\mathbf{b_u}} \quad & (P_I - P_V)(cs_0 + s) + \frac{s_0+s}{1-\rho'}[\sum_{j=1}^{c} P_{Tx,j}\rho_{u,j} + \\
& c(P_R - P_V)\rho_D + P_V\sum_{j=1}^{c}(1-\rho_{u,j})]. \\
s.t. \quad & \lambda_D\overline{b_D} + \sum_{j=1}^{c}\lambda_{u,j}b_{u,j} - 1 \leq 0. \\
& \frac{H_i}{\log_2(P_{max}/K_i)} - b_{u,i} \leq 0, \ \forall i. \\
& b_{u,i} - \frac{H_i}{\log_2(P_{min}/K_i)} \leq 0, \ \forall i. \\
& \frac{H_i}{\log_2 P_{MAX}/K_i} - b_{d,i} \leq 0, \ \forall i. \quad (17)
\end{aligned}$$

By introducing the downlink ratio $\beta_i = \lambda_{d,i}/\lambda_i$ as before, we have $\lambda_D = \sum_{j=1}^{c}\beta_j\lambda_j$, and $\lambda_{u,i} = (1-\beta_i)\lambda_i$, where λ_i is the total traffic sent from and received by q_i. Similar to the MG schedule, we have two special cases: $\boldsymbol{\beta} = \mathbf{0}$ and $\boldsymbol{\beta} = \mathbf{1}$. There are therefore $2c$ decision variables ($b_{d,i}$ and $b_{u,i}, i = 1, \ldots, c$) involved in the optimization formulation. We can reduce the number of the decision variables to c by considering the result in Prop. 3. As a result, the last constraint in (17) can be removed.

PROPOSITION 3. *In an optimal PG schedule, the AP transmits data with its maximal power P_{MAX}.*

PROOF. Note that $\mathbf{E}[E_{PG}]$ increases monotonically with $\overline{b_D}$, because both ρ_D and ρ' increase with $\overline{b_D}$. Therefore, the optimal downlink power allocation is obtained by $\overline{b_D^*} = (1/\lambda_D)\sum_{j=1}^{c}\lambda_{d,j}b_{d,j}^*$, where $b_{d,i}^* = \frac{H_i}{\log_2 P_{MAX}/K_i}, \forall i$. That is, the AP uses the maximal power to transmit. □

Similar to the MG schedule, we use the KKT conditions to obtain the necessary condition for an optimal PG schedule, which is stated in Proposition 4.

PROPOSITION 4. *If all wireless devices do not transmit data using their extreme power, $\mathbf{b_u}^*$ must satisfy $\mathbf{L}(\mathbf{b_u^*}) = \mathbf{R}(\mathbf{b_u^*})$ in an optimal PG schedule.*

PROOF. Let $\rho_D^* = \overline{b_D^*}\lambda_D$. $\mathbf{b_u}^*$ is a local minimum only when (18)-(21) are satisfied for a set of lagrangian multipliers $\{u^* \leq 0, \mathbf{v}^* \leq \mathbf{0}, \boldsymbol{\sigma}^* \leq \mathbf{0}\}$. Let $L_i(\mathbf{b_u}) = P_{Tx,i}(b_{u,i})(1-\rho) + \sum_{j=1}^{c}\rho_{u,j}P_{Tx,j}(b_{u,j}) + P_V(c-1+\rho_D)$, and $R_i(\mathbf{b_u}) = P_{Tx,i}(b_{u,i})(1-\rho)\ln(\frac{P_{Tx,i}(b_{u,i})}{K_i})$. The KKT conditions are given by:

$$\frac{\mathbf{E}[C]\lambda_{u,i}[L_i(\mathbf{b_u^*}) - R_i(\mathbf{b_u^*})]}{(1-\sum_{j=1}^{c}\lambda_j b_{u,j}^* - \rho_D^*)^2} - u^*\lambda_{u,i} + v_i^* - \sigma_i^* = 0, \ \forall i. \quad (18)$$

$$u^*(\rho_D^* + \sum_{j=1}^{c}\lambda_{u,j}b_{u,j}^* - 1) = 0, \quad (19)$$

$$v_i^*(\frac{H_i}{\log_2(P_{max}/K_i)} - b_{u,i}^*) = 0, \ \forall i. \quad (20)$$

$$\sigma_i^*(b_{u,i}^* - \frac{H_i}{\log_2(P_{min}/K_i)}) = 0, \ \forall i. \quad (21)$$

Obviously, $u^* = 0$ according to (19). If $P_{min} < P_i^* < P_{max}$, we have $v_i^* = \sigma_i^* = 0$ from (20) and (21). As a result, we have $L_i(\mathbf{b_u^*}) - R_i(\mathbf{b_u^*}) = 0, \ \forall i$ from (18). □

PROPOSITION 5. *In the pure downlink case,* $\mathbf{E}(E_{PG}) > \mathbf{E}(E_{MG})$ *with the same downlink transmission rates.*

PROOF. When $\boldsymbol{\beta} = \mathbf{1}$, $b_{u,i} = 0, \forall i$, and $\rho = \rho_D$. Using the same $b_{d,i}$, $\mathbf{E}(E_{PG}) - \mathbf{E}(E_{MG})$ is given by

$$cP_I s_0 + \frac{\rho_D}{1-\rho_D}[(cP_R - P_V)s_0 + ((c-1)P_R - cP_V)s] > 0,$$

because $P_R \gg P_V$ in practice. In particular, $\mathbf{E}^*(E_{PG}) > \mathbf{E}^*(E_{MG})$ when the AP transmits data with P_{MAX} and the same $b^*_{d,i}$ according to Props. 1 and 3. □

5.3 An iterative algorithm

We design iterative algorithms based on the results in Prop. 2 and Prop. 4 for the MG and PG schedules, respectively. In the following we use the MG schedule as an example to illustrate how the iterative algorithms work.

Calculate $\mathbf{b}_{min}$ and $\mathbf{b}_{max}$;
Choose ϵ_1, ϵ_2, d, $m = 0$, and then determine $\mathbf{P}^0_{Tx}$;
Initialize $\mathbf{L}(\mathbf{b}^m) \neq \mathbf{R}(\mathbf{b}^m)$;
While $|\frac{Norm(\mathbf{L})}{Norm(\mathbf{R})} - 1| < \varepsilon_1$ or $|\frac{\mathbf{L}^T\mathbf{R}}{Norm(\mathbf{L})Norm(\mathbf{R})}| > 1 - \varepsilon_2$
  $m = m + 1$;
  for $i = 1 : c$
    if $i = 1$
      $l_i = L_i(\mathbf{b}^{m-1}, \mathbf{P}^{m-1})$; $r_i = R_i(\mathbf{b}^{m-1}, \mathbf{P}^{m-1})$;
    else
      $l_i = L_i([b^m_{t(t<i)}, b^{m-1}_{t(t\geq i)}], [P^m_{t(t<i)}, P^{m-1}_{t(t\geq i)}])$; $(t = 1, \ldots, c)$
      $r_i = R_i([b^m_{t(t<i)}, b^{m-1}_{t(t\geq i)}], [P^m_{t(t<i)}, P^{m-1}_{t(t\geq i)}])$;
    end if
    if $r_i < l_i$, $b^m_i = \max\{(1-d)b^{m-1}_i, b_{min,i}\}$; end if
    if $r_i > l_i$, $b^m_i = \min\{(1+d)b^{m-1}_i, b_{max,i}\}$; end if
    $P^m_i = K_i 2^{\frac{H_i}{b^m_i}}$;
  end for
end while

We first determine the feasible region of the mean service times, which is bounded by $\mathbf{b}_{min}$ and $\mathbf{b}_{max}$. According to the power constraints $[P_{min}, P_{max}]$, the range of the decision variables must be within $[b^P_{min,i}, b^P_{max,i}]$ $\forall i$, as derived from (6). According to the stability constraint, we can obtain the minimum (maximum) average service time for any q_i, when other queues adopt $b^P_{max,j}$ ($b^P_{min,j}$), $j \neq i$, as $b^\rho_{min,i} = (1 - \sum_{j\neq i} \lambda_j b^P_{max,j})/\lambda_i$ ($b^\rho_{max,i} = (1 - \sum_{j\neq i} \lambda_j b^P_{min,j})/\lambda_i$). By combining the stability constraint with the power constraints, the feasible region is therefore given by $b_{min,i} = \max\{b^\rho_{min,i}, b^P_{min,i}\}$, and $b_{max,i} = \min\{b^\rho_{max,i}, b^P_{max,i}\}$. Given $\boldsymbol{\lambda}$, note that an decrease in P_{min} (P_{max}) will increase $b^P_{max,i}$ ($b^P_{min,i}$), but decrease $b^\rho_{min,i}$ ($b^\rho_{max,i}$). That is, $b_{min,i}$ is more likely to be determined by P_{max}, but $b_{max,i}$ is more likely to be determined by the stability constraint instead. Moreover, given $[P_{min}, P_{max}]$, $\mathbf{b}^\rho{}_{max}$ decreases with $\boldsymbol{\lambda}$; therefore, $\mathbf{b}_{max}$ will be more likely determined by the stability constraint. On the other hand, $\mathbf{b}_{min}$ is more likely determined by P_{max} when $\boldsymbol{\lambda}$ decreases.

Next we consider the main loop of the algorithm. Let $\mathbf{b}^m$ be the vector of the mean service rates at the beginning of mth iteration. We set $\mathbf{b}^0 = \mathbf{b}_{min}$, and $\mathbf{P}^0_{Tx}$ can be computed from (6). From Prop. 2, the ideal terminating condition is $\mathbf{L}(\mathbf{b}^m) = \mathbf{R}(\mathbf{b}^m)$. To obtain a close-enough condition, we exploit the fact that two vectors in the Euclidean space are the same if their norms are the same and the angle between them is zero. Therefore, given the accuracy tolerance parameters ε_1 and ε_2, the algorithm terminates when $|\frac{Norm(\mathbf{L})}{Norm(\mathbf{R})} - 1| < \varepsilon_1$ and $|\frac{\mathbf{L}^T\mathbf{R}}{Norm(\mathbf{L})Norm(\mathbf{R})}| > 1 - \varepsilon_2$. When ε_1 is near zero, the norms of $\mathbf{L}$ and $\mathbf{R}$ should be very close to each other. When ε_2 is near zero, $\cos\angle(\mathbf{L}, \mathbf{R})$ should be close to 1. Inside the iterative loop, R_i decreases monotonically with b_i (from (16)). Therefore, in the mth iteration for q_i, if $R_i > L_i$, we increase b^{m-1}_i by $d \in (0, 1)$, the step size; otherwise, b^m_i is decreased by d. Although the algorithm's complexity has not been proven, our extensive experiments show that it converges quickly, i.e. $m \leq 50$ in most cases. Furthermore, we have applied the idea of Gauss-Siedel iteration to reduce the convergence time.

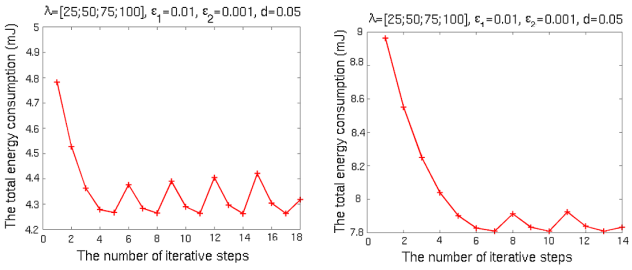

(a) MG schedule, $\boldsymbol{\beta} = 0.5e_4$ (b) PG schedule, $\boldsymbol{\beta} = 0.5e_4$

Figure 5: Energy consumption at iterative steps

When $c = 2$, both objective functions are convex within the stability area, as shown in Figure 6. In this case the iterative algorithm gives a single optimal solution. However, the objective functions are not convex for $c > 2$. As a result, the algorithm may return more than one local optimal solution. For these cases we select the one, whose objective function's value is the smallest, to be the optimal solution. Thus, the optimal transmission power allocations ($\mathbf{P}^*$) can be obtained from (6). As shown in Figure 5(a), for example, the iterative algorithm reaches several local minimums for the MG schedule, and the final optimal solution is obtained at the 14th iterative step.

The PG schedule has a similar iterative algorithm as the MG schedule, but has different $\mathbf{L}(\mathbf{b}^m)$ and $\mathbf{R}(\mathbf{b}^m)$. The feasible region $[\mathbf{b}_{min}, \mathbf{b}_{max}]$ is given by $b_{min,i} = \max\{(1 - \rho^*_D - \sum_{j\neq i} \lambda_j b^P_{max,j})/\lambda_i, b^P_{min,i}\}$ and $b_{max,i} = \min\{(1 - \rho^*_D - \sum_{j\neq i} \lambda_j b^P_{min,j})/\lambda_i, b^P_{max,i}\}$. Moreover, the PG optimal solutions include $\mathbf{b_u}^*$ which determines $\mathbf{P}^*_{Tx}$ for the wireless nodes, as well as $\mathbf{P}^*_{AP} = P_{MAX} \times e_c$ for the AP. Figure 5(b) shows the steps executed by the iterative algorithm.

6. PERFORMANCE EVALUATION

The experiment results presented in this section are based on $W = 1MHz$, $P_R = 2W$, $P_I = 1W$, and $P_V = 0.05W$, and the power constraints are given by $P_{MAX} = P_{max} = 10W$ and $P_{min} = 1W$.

6.1 Evaluation: model and algorithm

We first evaluate the performance of the iterative algorithm proposed in the last section. We will show that the algorithm can compute power allocations that are very close to the optimal ones. For the purpose of estimating the optimal power allocations, we have employed an exhaustive search method which divides the range of each average service time $[b_{min,i}, b_{max,i}]$ $\forall i$ evenly into n parts. For all the

possible n^c vectors of average service times, we first select those that satisfy the stability requirement and then find the one with the minimal energy consumption. Since the method is very time consuming, we have carried it out only for $c = 1, \ldots, 5$.

We first consider a case of 2 queues in Table 3 for both schedules. The results obtained from the iterative algorithm are marked by A ($d = 0.05$, $\varepsilon_1 = 0.01$ and $\varepsilon_2 = 0.001$). The results obtained from the exhaustive search method are indicated by N. We compare the optimal power $\mathbf{P}^*$ obtained from the two methods by computing an error rate $e_P = \frac{norm(\mathbf{P}^*_\mathbf{A} - \mathbf{P}^*_\mathbf{N})}{norm(\mathbf{P}^*_\mathbf{N})} \times 100\%$. The results show that the iterative algorithm yields optimal solutions that are very close to, if not the same as, the exact ones obtained by the exhaustive search. Besides the optimal results, the table also shows the number of iterative steps required by the iterative algorithm, denoted as m and the loc^{th} iteration at which the optimal solution is obtained. When $loc = m$, $\mathbf{b_u}$ is determined by $\mathbf{P}_{min}$ or $\mathbf{P}_{max}$. When $loc = m - 1$, the iteration stops after the first local solution is found, i.e. the m^{th} step leads to a higher energy consumption. Therefore, the single local solution is the global optimal and both objective functions are convex when $c = 2$.

The results for $c = 3, 4, 5$ are given in Table 4 and Table 5 for the MG schedule and the PG schedule, respectively. Note that $\boldsymbol{\beta} = k * e_c$. For example, the case of $k = 0.5$ represents a 50-50 mix of the uplink and downlink traffic. Once again the iterative algorithm yields quality solutions. Besides, if $\boldsymbol{\lambda}$ is small, then the initial workload $\boldsymbol{\rho}^{(0)}$ is very small. The final optimal solution is determined by $\mathbf{P}_{min}$ when the optimal workload $\lambda^T \mathbf{b}_{max}$ is also small. For example, in the 5-queue system with a light workload, the optimal transmission power allocation for the PG schedule is [1;1;1;1;1]. However, if the traffic rates are very high, $\boldsymbol{\rho}^{(0)}$ is close to $\mathbf{1}$. Then the wireless devices should send packets as fast as possible, i.e. the packets are transmitted with the maximal power allowed. For example, the optimal power allocation for the MG schedule is $\mathbf{P}_{max}$ when $\boldsymbol{\lambda} = [50; 100; 100; 150]$.

6.2 A comparison of the MG and PG schedules

Figure 6 presents the energy consumption obtained from an exhaustive search method in 3 different workload scenarios: light (Fig 6(a)), moderate (Fig 6(b)), and heavy (Fig 6(c)). For both schedules, $\mathbf{E}(E)$ is shown to be a convex function of the average service time when $c = 2$. The vertical lines in these figures locate the optimal solutions. Moreover, when the traffic arrival rate is too low or too high in reference to the power limitations, the optimal service rate could be determined by P_{min} or P_{max}, e.g. $\mathbf{P}^* = [1; 1]$ in the PG schedule when $\boldsymbol{\lambda} = [30; 60]$ and $\boldsymbol{\beta} = 0.3 \times e_2$.

In most cases, $\mathbf{E}(E_{MG}) < \mathbf{E}(E_{PG})$ within the stability region, except when $\boldsymbol{\lambda}$ is high enough. For example, in Figure 6(c), $\mathbf{E}(E_{MG}) > \mathbf{E}(E_{PG})$ when the elements of $\mathbf{b_u}$ are close to the upper boundary. The reason is that the MG schedule approaches much closer to its stability boundary which leads to a very long cycle period. In this case, the MG schedule consumes much more energy due to the long cycle. Furthermore, we repeat the experiments with different $\boldsymbol{\beta}$ by changing k from 0 to 0.9, and the values of $\frac{E^*_{MG}}{E^*_{PG}}$ are given in Figure 6(d). As shown, the optimal energy consumption for the MG schedule is always lower than the PG schedule's, i.e., $\frac{\mathbf{E}^*(E_{MG})}{\mathbf{E}^*(E_{PG})} < 1$. Therefore, the MG schedule is indeed more energy-efficient, especially when the proportion of the downlink traffic increases.

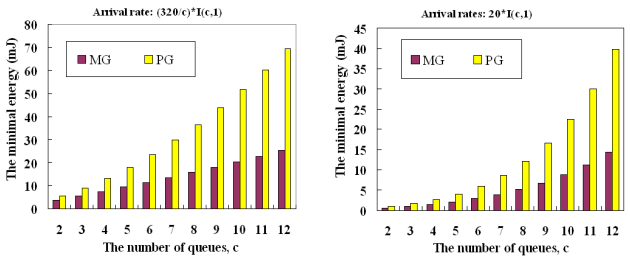

(a) $\sum_{i=1}^{c} \lambda_i = 320$, $k = 0.5$ (b) $\lambda_i = 20\ \forall i$, $k = 0.5$

Figure 7: Minimal energy consumption v.s. c

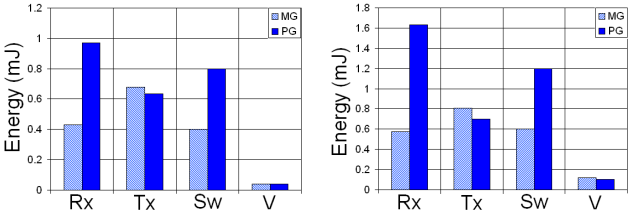

(a) $\boldsymbol{\lambda}$ =[60;100], $c = 2$ (b) $\boldsymbol{\lambda}$=[30;60;90], $c = 3$

Figure 8: Breakdown of energy consumption, $k = 0.5$

Moreover, we use the iterative algorithm to compare the energy efficiencies of the MG and PG schedules for $c > 2$. Figure 7 compares the minimal energy consumption for the two schedules with different traffic patterns. Again, they show that the optimal MG schedule can save more energy than the optimal PG schedule, which is consistent with the result in Prop. 5. Furthermore, the gap between the two schedules increases with the number of devices.

Finally, we identify the factors that are responsible for the MG schedule's high energy efficiency. To do so, we decompose the total energy consumption into the 4 components—energy due to receptions (Rx), transmissions (Tx), mode transitions (SW), and sleeping (V). We plot the results for both schedules in Figure 8. It is clear that the MG schedule is able to save a significant amount of energy during the reception and mode transition phases. Since the PG schedule broadcasts the downlink traffic, all wireless devices have to be in the active mode, thus consuming a much larger amount of energy. Moreover, each device in the PG schedule performs more mode transitions. As for the energy consumed during the transmission and sleeping mode, the two schedules consume almost the same amount of energy.

6.3 The delay analysis

In this section, we study how the delay performance is impacted by the optimal power allocation. The delay is defined to be the duration from the packet arrival to a queue to its departure from the queue, i.e., the queuing delay. However, it is not reasonable if we compare our optimal design with the energy efficient schemes in the term of delay performance. Therefore, we use simulations to compare the delay of the optimal MG with the delay of the PG schedule, and then compare the packet delay of each schedule with and without the optimal power allocations.

Table 3: Energy efficiency results for both MG and PG schedules, and $c = 2$, $\mathbf{E}[\mathbf{F}] = [1024; 512]$ bytes, $[N_1, N_2] = [0.02, 0.01]W$, $[g_{11}, g_{12}] = [6, 8]$, and $\alpha = 0.7$.

Schedule	$\boldsymbol{\lambda}(packets/s)$	$\boldsymbol{\beta}$	$[b_1^*; b_2^*](ms/packet)$	$\mathbf{P}^*(W)$	$e_P(\%)$	ρ^*	m	loc	$\mathbf{E}^*(E)$(mJ)
MG (N)	[30;60]	[0;0]	[7.6517;3.2117]	[1.000,1.000]	–	0.4223	–	–	0.7270
MG (A)	[30;60]	[0;0]	[7.6517;3.2117]	[1.000,1.000]	0	0.4223	16	16	0.7270
MG (N)	[60;100]	[0.3;0.3]	[5.3014;2.4305]	[2.5600;2.2518]	–	0.5611	–	–	1.6211
MG (A)	[60;100]	[0.3;0.3]	[5.3121;2.4330]	[2.5443;2.2442]	0.5100	0.5620	21	20	1.6211
MG (N)	[60;150]	[0.6;0.6]	[4.3852;2.0170]	[4.8520;4.4637]	–	0.5657	–	–	2.0389
MG (A)	[60;150]	[0.6;0.6]	[4.3922;2.0117]	[4.8234;4.5116]	0.8500	0.5653	14	13	2.0391
Schedule	$\boldsymbol{\lambda}(packets/s)$	$\boldsymbol{\beta}$	$[b_{u,1}^*; b_{u,2}^*](ms/packet)$	$\mathbf{P}^*(W)$	$e_P(\%)$	ρ^*	m	loc	$\mathbf{E}^*(E)$(mJ)
PG (N)	[30;60]	[0;0]	[7.6517;3.2117]	[1.000,1.000]	–	0.4223	–	–	1.2804
PG (A)	[30;60]	[0;0]	[7.6517;3.2117]	[1.000,1.000]	0	0.4223	16	16	1.2804
PG (N)	[60;100]	[0.3;0.3]	[6.0981;2.7828]	[1.7163;1.4759]	–	0.5673	–	–	2.5054
PG (A)	[60;100]	[0.3;0.3]	[6.0629;2.7769]	[1.7430;1.4851]	1.2500	0.5654	18	17	2.5054
PG (N)	[60;150]	[0.6;0.6]	[5.6201;2.5684]	[2.1521;1.8825]	–	0.5722	–	–	3.2436
PG (A)	[60;150]	[0.6;0.6]	[5.6057;2.5675]	[2.1682;1.8847]	0.5700	0.5718	19	18	3.2436

Table 4: Energy efficiency results for the MG schedule and $c > 2$

Methods	$\boldsymbol{\lambda}(packets/s)$	$\mathbf{b}^*(ms/packet)$	$\mathbf{P}^*(W)$	$e_P(\%)$	ρ^*	$\rho^{(0)}$	$\mathbf{E}^*(E)$(mJ)
N	[30;60;90]	[4.9960;2.2154;2.2927]	[3.0340;2.6753;2.7521]	–	0.4891	–	2.0997
A	[30;60;90]	[5.0087;2.2106;2.2940]	[3.0612;2.6156;2.7464]	1.3500	0.4894	0.3584	2.0997
N	[60;100;140]	[4.0096;1.8156;1.8551]	[7.0220;5.8684;6.2119]	–	0.6813	–	6.1787
A	[60;100;140]	[4.0441;1.8050;1.8731]	[6.6286;5.9663;6.0794]	3.8600	0.6854	0.6172	6.1784
N	[25;50; 75;100]	[4.6242;2.0594; 2.0594;2.1089]	[4.0075;3.4242; 3.4242;3.7462]	–	0.5839	–	4.2634
A	[25;50;75;100]	[4.6118;2.0354; 2.0354;2.1123]	[4.0455;3.5870; 3.5870;3.7234]	3.2000	0.5809	0.4621	4.2625
N or A	[50;100;100;150]	[3.6681;1.6189; 1.6189;1.6800]	[10;10;10;10]	0	0.7592	0.7592	16.4317
N or A	[5;10;15;20;25]	[5.7982;2.5590;2.5590; 2.5590;2.6556]	[1.9695;1.5870;1.5870; 1.5870;1.6969]	0	0.2105	0.1248	1.7433
N	[20;30;50;70;90]	[4.4648;2.0319;2.0319; 2.0319;2.1395]	[4.5420;3.6119;3.6119; 3.6119;3.5454]	–	0.5866	–	5.5509
A	[20;30;50;70;90]	[4.5658;2.0151;2.0151; 2.0151;2.0912]	[4.1912;3.7338;3.7338; 3.7338;3.8701]	5.1441	0.5818	0.4382	5.5472

Table 5: Energy efficiency results for the PG schedule and $c > 2$

Methods	$\boldsymbol{\lambda}(packets/s)$	$\mathbf{b_u}^*(ms/packet)$	$\mathbf{P}_{Tx}^*(W)$	$e_P(\%)$	ρ^*	$\rho^{(0)}$	$\mathbf{E}^*(E)$(mJ)
N	[30;60;90]	[6.0583;2.6284;2.7522]	[1.7466;1.4597;1.5245]	–	0.4728	–	3.6379
A	[30;60;90]	[5.9750;2.6370;2.7366]	[1.8121;1.4441;1.5503]	2.6600	0.4711	0.3584	3.6377
N	[60;100;140]	[4.4648;2.0319;2.0885]	[4.5420;3.6119;3.8897]	–	0.6903	–	10.1305
A	[60;100;140]	[4.5430;2.0051;2.0808]	[4.2666;3.8100;3.9462]	4.9200	0.6908	0.6172	10.1291
N	[25;50;75;100]	[5.1022;2.2796; 2.2796;2.3540]	[2.8848;2.3404; 2.3404;2.5100]	–	0.5550	–	7.8092
A	[25;50;75;100]	[5.1100;2.2553; 2.2553;2.3404]	[2.8708;2.4321; 2.4321;2.5605]	2.7700	0.5529	0.4621	7.8089
N or A	[50;100;100;150]	[3.6681;1.6189; 1.6189;1.6800]	[10;10;10;10]	0	0.7592	0.7592	30.3315
N or A	[5;10;15;20;25]	[7.5121;2.9954;2.9954; 2.9954;3.2117]	[1;1;1;1;1]	0	0.1929	0.1248	3.4167
N	[20;30;50;70;90]	[4.9960;2.1695;2.1695; 2.1695;2.2927]	[3.0866;2.8037;2.8037; 2.8037;2.7521]	–	0.5495	–	10.9766
A	[20;30;50;70;90]	[4.9157;2.1695;2.1695; 2.1695;2.2514]	[3.2548;2.8038;2.8038; 2.8038;2.9365]	3.9131	0.5469	0.4382	10.9749

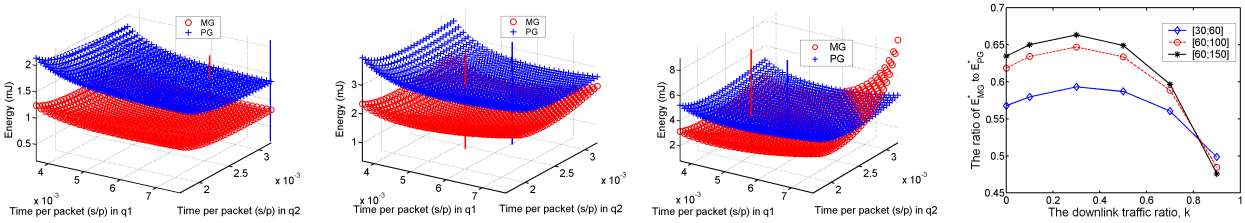

(a) $\lambda = [30; 60], k = 0.3$ (b) $\lambda = [60; 100], k = 0.3$ (c) $\lambda = [60; 150], k = 0.3$ (d) E^*_{MG}/E^*_{PG} v.s. k

Figure 6: Comparing the energy efficiency for PG and MG schedules and $c = 2$

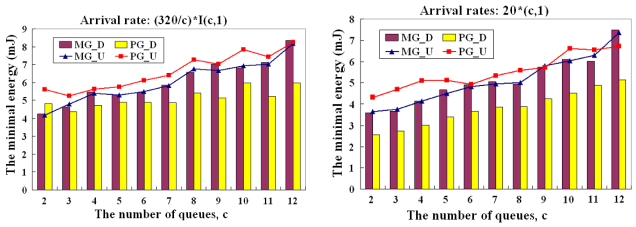

(a) $\sum_{i=1}^{c} \lambda_i = 320$, $k = 0.5$ (b) $\lambda_i = 20$, $k = 0.5$

Figure 9: Delay comparison under optimal schedules

6.3.1 *Average delay under optimal power allocations*

The simulation yields the average packet delay under different optimal power allocations. Denote the average delay of the downlink packets by $\mathbf{T_D}$ and that for the uplink packets by $\mathbf{T_U}$, and the total energy consumed per the polling cycle by $\overline{E}$. For $c = 4$, the average delay of the downlink packets and uplink packets under the optimal power allocation are shown in Table 6, where $\sigma_T = \sum_{i=1}^{c}(T_i - \overline{T})^2/c$ is the delay variance, and $\overline{T} = \sum_{i=1}^{c} T_i$. Three traffic workloads of $\boldsymbol{\lambda} = [10; 15; 20; 25] \times x$, $x = 1, 3, 5$, and $\boldsymbol{\beta} = 0.5e_4$ are considered and the packet size is 512 bytes. Clearly, the optimal MG schedule consumes less average energy per cycle than the corresponding optimal PG schedule. The small σ_T values show that the four queues with different arrival rates have similar delay. In other words, the optimal power allocations do not adversely affect the delay fairness. For all optimal PG schedules, the average delay of uplink packets are longer than that for the downlink packets. Additionally, their downlink delay increases with x.

In order to simplify the delay analysis, we simulate the optimal power allocation in a symmetric network with $\boldsymbol{\lambda} = ke_c$ and $\boldsymbol{\beta} = 0.5e_c$, $c = 2, \ldots, 12$, and the results are shown in Figure 9. The average delay for the downlink is $\overline{T_D} = \sum_i^c T_{D,i}/c$ and the average delay time for the uplink is $\overline{T_U} = \sum_i^c T_{U,i}/c$. $\overline{T_D}$ is close to $\overline{T_U}$ in all optimal MG schedules, while $\overline{T_D}$ is less than $\overline{T_U}$ in all optimal PG schedules. In most cases, the optimal PG schedules have lower delay for the downlink packets than the optimal MG schedules, while the optimal MG schedules have the lower delay for the uplink packets than the optimal PG schedules. Therefore, the optimal PG schedule may provide the better delay performance when β increases, and the optimal MG schedule may provide the better delay performance when β decreases.

6.3.2 *Energy efficiency v.s. delay*

We investigate the relationship between the energy efficiency and the delay performance. We still consider the symmetric system with $\boldsymbol{\lambda} = 20e_c$ and $\boldsymbol{\beta} = 0.5e_c$ with the MG and PG schedules. Without the optimal power allocation, we use a random power allocation which selects a power allocation randomly from the feasible region $[\mathbf{b}_{min}, \mathbf{b}_{max}]$. For these nonoptimal power allocations, we define 2 quantities in reference to the energy and delay obtained for the optimal power allocation. Define the *energy inflation ratio* (r_e) of a random allocation by $\frac{\overline{E}-\overline{E^*}}{\overline{E^*}}$, where $\overline{E^*}$ and $\overline{E}$ are the energy consumption obtained from the optimal power allocation and the random power allocation, respectively. Similarly, we define the *delay inflation ratio* (r_d) of a random allocation by $\frac{\overline{T_D}-\overline{T_D^*}}{\overline{T_D^*}}$ and $\frac{\overline{T_U}-\overline{T_U^*}}{\overline{T_U^*}}$ for the downlink and uplink traffic, respectively.

Figure 10 depicts the results for 60 random allocations with $c = 4$. Both the optimal MG and PG schedules definitely achieve the minimal energy consumption, because all the energy inflation ratios are positive, i.e. $r_e \geq 0$. However, neither the optimal MG schedule nor the optimal PG schedule can achieve the best delay performance, because some of the delay inflation ratios are negative.

We divide each figure in Figure 10 into 4 regions: Z_1 ($r_d > r_e$), Z_2 ($0 < r_d < r_e$), Z_3 ($-r_e < r_d < 0$), and Z_4 ($r_d < -r_e$). The random allocations in Z_1 and Z_2 have the longer delay than the optimal allocation, i.e. $r_d > 0$. Therefore, the optimal allocation outperforms the random allocations in these 2 regions on both energy efficiency and delay performance. On the other hand, the random allocations in Z_3 and Z_4 have better delay performance than the optimal allocation. However, trading the delay for energy efficiency may still be justified in Z_3, because the energy inflation ratio is always higher than the delay inflation ratio in this region, i.e. $|r_d| < r_e$. Figure 10 shows that most of the random allocations fall into Z_1 and Z_2 (at least 94%). Only a small percentage (at most 6%) of the random allocations belong to Z_4. As a result, we can conclude that both schedules can achieve optimal power allocation without the expense of a higher average delay most of the time.

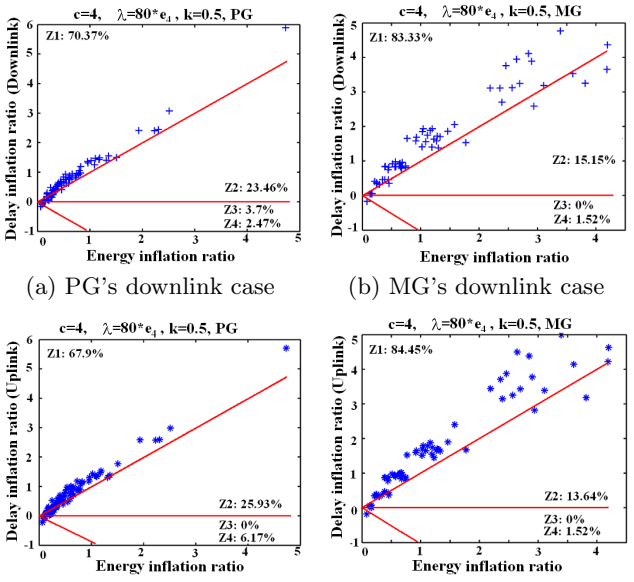

(a) PG's downlink case (b) MG's downlink case

(c) PG's uplink case (d) MG's uplink case

Figure 10: Energy inflation ratio and delay inflation ratio for a random power allocation, $c = 4$.

7. CONCLUSIONS AND FUTURE WORK

In this paper we have considered the problem of optimizing energy efficiency for *all* wireless devices in a polling-based wireless network. We have employed both the power saving mode (PSM) and the transmission power control (TPC) to conserve energy. Since the decrease in one's transmission power could adversely affect other devices, we have formulated an optimization problem to minimize the energy con-

Table 6: The average delay obtained from simulation for $\boldsymbol{\lambda} = [10; 15; 20; 25] \times x$ and $\boldsymbol{\beta} = 0.5e_4$

Scheduling	x	$\overline{E}(mJ)$	$\mathbf{T_U}(ms)$	σ_{TU}	$\mathbf{T_D}(ms)$	σ_{TD}
MG	1	1.3564	[4.0246;3.8502;4.1127;4.1467]	0.0132	[3.6882;4.1600;4.0260;4.1960]	0.0402
MG	3	3.5190	[4.7928;4.4650;4.9875;4.6139]	0.0383	[4.5765;5.0436;4.4353;4.7767]	0.0523
MG	5	9.2480	[5.0329;4.3240;4.8556;5.2596]	0.1192	[4.3194;4.7842;4.7272;4.9750]	0.0571
PG	1	2.6617	[5.3914;5.1583;4.9916;4.9916]	0.0265	[2.8538;2.8861;2.7985;3.3033]	0.0402
PG	3	6.6091	[5.3249;5.0583;5.6859;5.0535]	0.0668	[3.8474;4.1120;3.9285;4.1517]	0.0163
PG	5	15.4546	[5.0577;5.8118;6.4648;5.6484]	0.2511	[4.8643;5.2513;5.0549;4.7520]	0.0361

sumed during a polling cycle and, at the same time, ensure that all devices are stable, i.e., their queue lengths would not go unbounded. The resulted stability-constrained optimization formulation enables us to compute the optimal power allocations for 2 polling schedules—phase grouping and mobile grouping. The experiment results have shown that the mobile grouping schedule is much more energy efficient, because it decreases the number of mode transitions and allows a device to sleep for a longer time. Using simulation, we have also investigated the impact of the optimal power allocations on the queueing delay. The results show that the optimal power allocation does not degrade the delay for over 90% of the time. Even when the average delay becomes longer, the tradeoff is still considered beneficial as a whole.

Acknowledgment

The work described in this paper was partially supported by a grant from the Research Grant Council of the Hong Kong Special Administrative Region, China (Project No. PolyU 5146/01E).

8. REFERENCES

[1] J. Chen, K. Sivalingam, and P. Agrawal, "Performance comparison of battery power consumption in wireless multiple access protocols," *ACM/Baltzer Wireless Networks*, vol. 5, no. 6, pp. 445–460, 1999.

[2] D. Ciao, S. Choi, A. Soomro, and K. Shin, "Energy-efficient PCF operation of IEEE 802.11a wireless LAN," in *Proc. IEEE INFOCOM*, 2002.

[3] S. Singh and C. Raghavendra, "PAMAS power aware multi-access protocol with signalling for ad hoc networks," *ACM Computer Communication Review*, vol. 28, no. 3, pp. 5–26, 1998.

[4] A. Tarello, J. Sun, M. Zafer, and E. Modiano, "Minimum energy transmission scheduling subject to deadline constraints," in *Proc. IEEE WIOPT*, 2005.

[5] F. Zhang and S. Chanson, "Throughput and value maximization in wireless packet scheduling under energy and time constraints," in *Proc. IEEE RTSS*, 2003.

[6] T. Holliday, A. Goldsmith, and P. Glynn, "Optimal power control and source-channel coding for delay constrained traffic over wireless channels," in *Proc. IEEE ICC 2002*.

[7] P. Nuggehalli, V. Srinivasan, and R. Rao, "Delay constrained energy efficient transmission strategies for wireless devices," in *Proc. IEEE INFOCOM*, 2002.

[8] C. Schurgers, V. Raghunathan, and M. Srivastava, "Modulation scaling for real-time energy aware packet scheduling," in *Proc. Global Communications Conference*, 2001, pp. 3653–3657.

[9] M. Chiang and J. Bell, "Balancing supply and demand of bandwidth in wireless cellular networks: Utility maximization over powers and rates," in *Proc. IEEE INFOCOM*, 2004.

[10] J. Chen, K. Sivalingam, P. Agrawal, and R. Acharya, "Scheduling multimedia services in a low-power MAC for wireless and mobile ATM networks," *IEEE Trans. multimedia*, vol. 1, no. 2, 1999.

[11] J. Havinga and J. Smit, "Energy-efficient wireless networking for multimedia applications," *Wireless Communications and Mobile Computing*, vol. 1, 2001.

[12] R. Haines and A. Aghvami, "Indoor radio environment considerations in selecting a media access control protocol for wideband radio data communications," in *Proc. IEEE ICC*, 1994.

[13] P. Havinga and G. Smit, "E2MaC: an energy efficient MAC protocol for multimedia traffic," University of Twente, Tech. Rep., 1998.

[14] P. Havinga, G. Smit, and M. Bos, "Energy efficient adaptive wireless network design," in *Proc. IEEE ISCC*, 2000.

[15] E. Biyikoglu, B. Prabhakar, and A. Gamal, "Energy-efficient packet transmission over a wireless link," *IEEE/ACM Trans. Networking*, vol. 10, no. 4, 2002.

[16] A. Gamal, C. Nair, B. Prabhakar, E. Biyikoglu, and S. Zahedi, "Energy-efficient scheduling of packet transmissions over wireless networks," in *Proc. IEEE INFOCOM*, 2002.

[17] D. Qiao, S. Choi, A. Jain, and K. Shin, "MiSer: An optimal low-energy transmission strategy for IEEE 802.11a/h," in *Proc. MobiCom 03*, 2003.

[18] S. Jayashree, B. Manoj, , and C. Murthy, "Next step in MAC evolution: Battery awareness?" in *Proc. IEEE Globecom*, 2004.

[19] M. Ferguson and Y. Aminetzah, "Exact results for nonsymmetric token ring systems," *IEEE Trans. Communications*, vol. 33, no. 3, pp. 223–231, March 1985.

[20] W. Szpankowski, "Stability conditions for some multiqueue distributed systems: buffered random access systems," *Adv. Appl. Probab.*, vol. 26, 1994.

[21] H. Takagi, "Queueing analysis of polling models: an update," *Stochastic Analysis of Computer and Communication Systems*, pp. 267–318, 1990.

[22] L. Foulds, *Optimization Techniques*. Springer-Verlag New York Inc., 1981.

[23] G. Koole and P. Nain, "An explicit solution for the value function of a priority queue," *Queueing Systems*, vol. 47, pp. 251–285, 2004.